JOURNAL OF OPTOELECTRONICS AND ADVANCED MATERIALS, Vol. 8, No. 6, December 2007, p. 2120 - 2125

Preparation of micro - and nanocrystalline CdSe and CdS thin films suitable for sensor applications*

D. NESHEVA[a*], Z. ANEVA[a], S. REYNOLDS[b,c], C. MAIN[c], A. G. FITZGERALD[c]
[a]*Institute of Solid State Physics, Bulgarian Academy of Sciences, 72 Tzarigradsko Chaussee Blvd., 1784 Sofia, Bulgaria.*
[b]*Institut für Photovoltaik, Forschungszentrum Jülich GmbH, D-52425 Jülich, Germany*
[c]*University of Dundee, Division of Electronic Engineering and Physics, Dundee DD1 4HN, UK*

Thin films of CdS (30-200 nm) and CdSe (10-100 nm) are prepared by physical vapour deposition using one-step (for CdS and CdSe) or step-by-step (for CdSe only) approach. Atomic force microscopy measurements reveal a grain size decrease with decreasing layer thickness. The effect is strongest in the step-by-step CdSe layers. Raman scattering measurements show an anticipated gradual increase of the scattered light from CdS layers with thickness and a non-monotonous change in the CdSe group, the intensity is strongest for the '50 nm' 'step-by-step' CdSe layer. This observation is ascribed to a size-induced increase of the optical band gap of a part of the microcrystals whose estimated size is ~ 8 nm. Room temperature investigations of the effect of exposure to a set of vapours (water, ethanol, ammonia, acetone, iodine) on the dc dark and steady state photoconductivity of CdS layers show a reasonable response of all CdS layers to water vapour. CdSe layers are rather insensitive with the exception of the '50 nm' layer, as the 'step-by-step' layer shows the best sensitivity to all vapours. The observed good gas-sensitivity of the 'step-by-step' CdSe layers is ascribed to a much greater integral interface area between nanocrystals and indicates that 'step-by-step' deposition of CdSe layers is quite promising for gas-sensor applications.

(Received October 10, 2006; accepted Novemeber 2, 2006)

Keywords: Thin films of CdS and CdSe, Physical vapour deposition, Atomic force microscopy, Dark and photoconductivity, Gas sensitivity

1. Introduction

Miniaturized solid-state chemical sensors play an important role in chemical processes controlling, pollutant monitoring, personal safety, medical diagnosis, and sensor networks. The use of semiconductors in gas sensor applications is well-established [1] because a number of properties of a semiconductor material can be changed by adsorbing chemicals. Since the gas sensing principle is associated with a surface phenomenon rather than with a bulk phenomenon, the trend is to develop gas sensors using thin film technology. With the recent development of nanoscience and nanotechnology attention has also been given attracted by nanostructured materials, as well. Because of the huge surface-to-volume ratio of nanoparticles and the high porosity of nanoparticle layers and assemblies, a large number of analyte molecules can be adsorbed by a nanoparticle and within a nanoparticle structure in a very short time. This leads to both a high sensitivity of the sensor comprising these nanoparticles as analyte-sensitive indicators as well as to a short response time [2-7]. Although the first results on nanoparticle assembly sensors are very promising, there still exist many problems with the reproducibility and mass production of such sensors. On the other hand, semiconductor gas sensors in the form of thin films are highly sensitive and reliable, having a performance/price ratio comparable to that of microelectronic components. Therefore, the work on thin film sensors, is still very active [8-10].

Semiconductor chemical sensors operate on the basis of analyte induced changes mainly in the film resistance, photoconductivity, optical absorption and fluorescence. The direct measurement of the changes in the electrical and optical properties in many chemical sensing applications is very convenient. When the property measured is the dark conductivity, which is governed by a combination of charge carrier density, and the carrier mobility, adsorbed gases cause a change in the carrier concentration by introducing donors or acceptors, by altering the concentration of electronic defects and by surface band-bending through the electrostatic effect of polar molecules. The presence of adsorbates also influences the photoconductive [11] and photoluminescent [12] properties of films such as CdS and CdSe by creating defects affecting the radiative and non-radiative recombination in the films [13 and reference therein]. Films of these two materials grown by physical evaporation technique have been used as gas sensors for the detection of oxygen [14].

In this article CdS and CdSe microcrystalline thin layers have been prepared by physical vapour deposition using one-step or step-by-step deposition approaches. The main task of this study is a search for deposition conditions and layer thickness of these films which ensure a good gas-sensitivity of the layers. Investigations of the

*Paper presented at the International School on Condensed Matter Physics, Varna, Bulgaria, September 2006

microcrystal size and electronic properties of the films have been carried out and the layer sensitivity to a number of gases has been tested. A useful relation has been ascertained between the CdSe film deposition conditions and the gas sensitivity of the films.

2. Experimental details

Microcrystalline single layers of CdSe having thickness of 10, 40, 50, 75 and 100 nm and CdS having thickness of 30, 50, 100 and 200 nm were deposited on Corning 7059 glass substrates held at 25 °C for CdSe and 150°C for CdS. The layers were produced by physical evaporation of powdered CdSe and CdS (Merck Suprapure) at a residual pressure of ~$3x10^{-4}$ Pa from tantalum crucibles located in the bottom of cylindrical screens (not intentionally heated). The top of the screens is close to the substrates, thus evaporation in a quasi-closed volume is carried out. A previously calibrated quartz microbalance system was used to control the nominal layer thickness and deposition rate (V_d = 0.5 nm/s, 2.5-3.0 nm/s) of both materials.

Two deposition approaches were applied: (i) the widely used one-step deposition, in which the substrates are maintained above the crucible, applied when depositing all CdS layers and a part of the CdSe ones or (ii) step by-step deposition in which the substrates were rotated spending only 1/12 part of the turn time over the CdSe source. During the step-by-step deposition the substrates were rotated at a rate of 8 turns/min. Thus, more than 25 'sublayers', with a nominal thickness of ~0.1-1.8 nm in each step, form the respective layer with 6.9 s between the steps. It should be noted that with this deposition geometry the growth of CdS layers, when using lower substrate temperatures or step-by-step deposition at 150 °C, was very slow and not easily reproduced and, for this reason, no investigations on such layers were performed.

As is well known, the gas sensitivity of semiconductor films is strongly affected by the film structure. The CdSe crystallite size, structure and spatial distribution were investigated using a Digital Instruments Dimension 3000 Scanning Probe Microscope in the tapping mode. For the electrical and photoelectrical measurements, carried out under an applied voltage of 10 V, samples were provided with 10 mm long, 1.5 mm spaced planar contacts from melted indium (99.99) on the top layer surface. All the contacts used were found to be Ohmic and to have symmetric behaviour with respect to the voltage polarity. The measurements were carried out in a low-vacuum cryostat (1 Pa) using a Keithley 610C Electrometer. In the photocurrent measurements samples were illuminated with white light (~30 mW/cm^2) from a tungsten halogen lamp using a filter that cuts out wavelengths λ>750 nm to avoid sample heating. Raman spectra were taken using the exciting line wavelengths quoted alongside the results.

In order to get qualitative information about the changes of the dc dark current (I_d) and steady state photocurrent (I_p) when exposing layers to ammonia, water vapour, ethanol, acetone vapour and saturated solution of iodine in ethanol (the carrier gas is air), the samples were put in the cryostat as shown schematically in Fig.1. First dark and then photocurrent values were measured at room temperature before and after exposure. Vapour content in the air entering the cryostat when opening the entrance valve was not strictly controlled. Its level was determined by the vapour drawn into the cryostat from a soaked piece of cloth fixed to the valve entrance. The exposure procedure described was repeated several times on each sample and a good reproducibility has been registered. Normally, the evacuation of the cryostat for a few minutes, up to 10 minutes (with an exception for iodine) was enough to return the sample in the initial state (i.e. to recover the initial I_d and I_p values) and sample heating was not necessary.

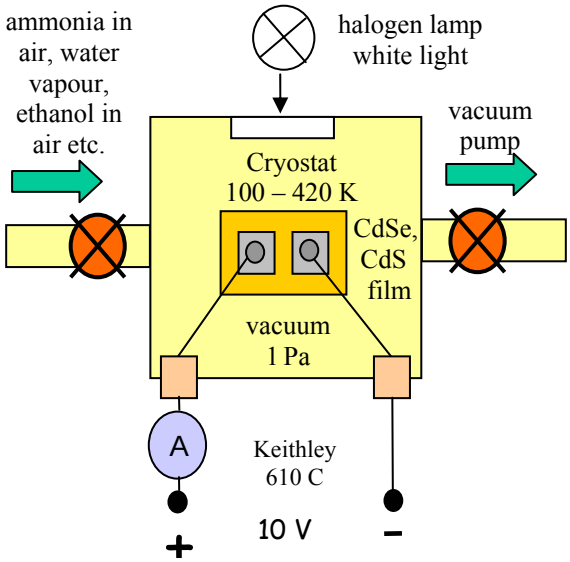

Fig. 1. Experimental set-up used for the measurement of dark current and steady state photocurrent when exposing layers to ammonia, water vapour, ethanol, acetone vapour and saturated solution of iodine in ethanol.

3. Results and discussion

Atomic force microscopy (AFM) images of two CdS layers having thickness of 100 and 50 nm are shown in Fig.2. Both layers have very smooth surfaces (~ 2 and 1.2 nm for the average roughness of a 2x2 μm area of the '100 nm' and '50 nm' layers, respectively; the AFM data are not shown here), which makes the determination of the exact size of the microcrystals rather difficult. Nevertheless, it seems that their size is relatively large, ~500 nm for the `100 nm' layers and roughly half this size in the '50 nm' ones i.e., as expected, the thinner the layer, the smaller the crystal size. Therefore, one can anticipate (a rise of) an increase in the gas sensitivity with decreasing layer thickness. The results presented in Table 1 are in good agreement with this anticipation for all gaseous materials used. Moreover, the sensitivity of the '200 nm' layer is less than that of the '100 nm' one. One can see from Table 1

that both the dark conductivity and photoconductivity exhibit the highest sensitivity to water and also a good sensitivity to ammonia. The changes in the dark current are much stronger than in the photocurrent.

A common model has been developed based on the fact that polycrystalline films consist of a large number of grains, contacting at their boundaries [15-16]. The electrical behaviour is governed by the formation of double Schottky potential barriers at the interface of adjacent grains, caused by charge trapping at the interface. The height of this barrier determines the conductance. When exposed to a chemically reducing gas, like ammonia, co-adsorption and mutual interaction between the gas and the oxygen result in oxidation of the gas at the surface. The removal of oxygen from the grain surface results in a decrease in barrier height and hence an increase of the dark current. The illumination of layers reduces the barrier height and the observed photocurrent changes, related to barrier variations, are normally smaller than the dark current ones. Such changes may be greater if the adsorbed gas atoms or molecules not only alter the barrier height but also introduce new recombination centres or change the relative concentration of the existing ones. It seems that in our CdS microcrystalline layers the first mechanism is predominant. Since the main purpose of this study was to search for both CdS and CdSe deposition conditions and layer thickness which ensure a good gas-sensitivity of the layers, these preliminary results on gas induced I_p and I_d changes are essentially qualitative, and detailed discussion of the mechanisms responsible is reserved for future investigations.

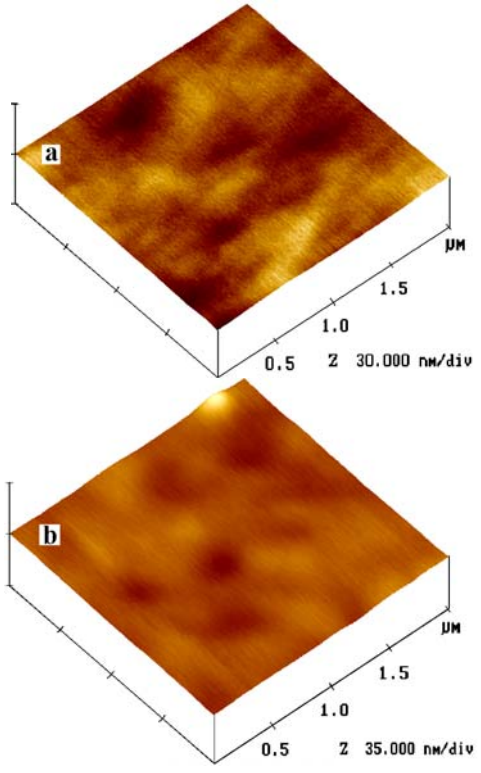

Fig . 2. Three dimensional AFM images of two 'one-step' CdS layers having thickness of 100 nm (a) and 50 nm (b).

A CdS thick film photoconductivity gas sensor has previously been reported for detection of hazardous gases in the enviroment[11]. A comparison of the data in Table 1 with these thick film devices shows that the observed photocurrent changes are comparable provided measurements on the thick film sensors were carried out at 200^{o}C at 200 Hz, which increases the gas response of the films, and in addition Pt has been used to sensitize the films.

In an attempt to increase further the gas sensitivity of the CdS films, their thickness was diminished down to 30 nm. A strong reduction of film photoconductivity was observed which can be related to: (i) introduction of new recombination centres due to decrease of microcrystal size and increase of the surface-to-volume ratio or (ii) to strengthening the role of adsorbed oxygen which acts as a fast recombination centre in CdS and thus strongly reduces the photocurrent. Similar results have been obtained when reducing CdSe layer thickness from 50 nm down to 10 nm. On the other hand, Se/CdSe [17] and SiO_x/CdSe [18] multilayers having a layer thickness ≤ 10 nm showed a good photosensitivity. Hence, the physical absorption of oxygen on the surface of the CdSe and CdS ultra thin layers is most likely more important for the observed strong reduction of the layer photosensitivity. The described thickness dependent photocurrent changes have indicated that the minimum layer thickness suitable for gas sensing experiments is 50 nm and therefore we do not report on thinner layers here.

Fig. 3 depicts AFM images of three CdSe layers having thickness of 100 nm, one-step (a - V_d=3.0 nm/s, b - V_d=0.5 nm/s) and step-by-step (c - V_d=0.5 nm/s) deposited. The images look very similar; the microcrystal size is ~260x130 nm for the one-step layers and ~200x100 nm for the step-by-step one.

Table 1 Changes in the steady state photocurrent and dark current of one-step deposited CdS thin films upon exposure at room temperature to different vapours in air. The signs (+) and (-) in front of the numbers indicate photocurrent increase or decrease, respectively.

Layer thickness (nm)	Photocurrent changes %			
	ammonia	water	ethanol	acetone
100	+25	+50	<-10	<-10
50	+50	+100	-20	-30
	Dark current changes %			
100	$+3x10^2$	$+10^6$	$+2x10^2$	+70
50	$+7x10^4$	$+10^6$	+45	+100

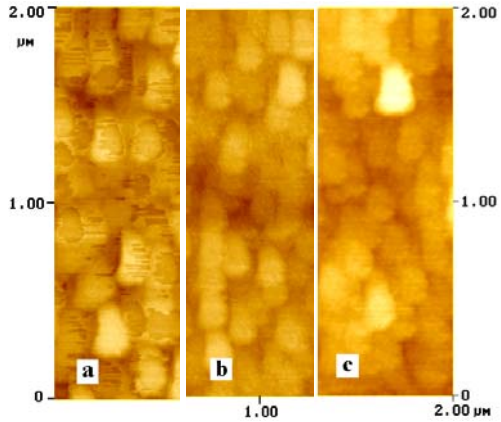

Fig. 3. Two-dimensional AFM images of three CdSe layers having thickness of 100nm prepared using one-step (a - V_d=3.0 nm/s, b - V_d=0.5 nm/s) and step-by-step (c-V_d=0.5 nm/s) deposition.

The results show that in the one-step layers the change of the deposition rate does not affect appreciably the grain size. At the same deposition rate the step-by-step deposition results in a smaller grain size though the observed decrease is not very strong. The microcrystal sizes are appreciably smaller than that of the '100 nm' and even '50 nm' CdS layers while the average roughness [19] is 3-4 times greater. This observation can be explained by the significantly lower substrate temperatures of CdSe layers. It is known [20] that the lower the temperature, the lower the mobility of adatoms, which results in a smaller crystal size.

Fig. 4 shows AFM images of three CdSe layers having thickness of 50 nm, deposited one-step (a - V_d=2.5 nm/s, b - V_d=0.5 nm/s) and step-by-step (c-V_d=0.5 nm/s). In contrast with the '100 nm' CdSe layers, these samples show a clear decrease of the microcrystal size both with decreasing deposition rate and with the change in the deposition procedure. It should be pointed out that the effect of the deposition procedure is stronger than that of the deposition rate; at same V_d the microcrystal size of the one-step deposited layer (~20-30 nm) is twice as large as in the step-by-step one (~10-15 nm). It has been ascertained [20] that at low deposition temperature the crystal grain size depends weakly on the deposition rate; at low deposition rates it slightly (<20 %) increases with the rate. These observations are in good agreement with the size increase displayed in Fig. 4 a, b. In fact the average deposition rate for the step-by-step layers is 0.04 nm/s and the observed ~100% microcrystal size decrease could be an expression of this dependence appearing at very low deposition rates. Most likely at the very beginning of the layer growth at room temperature the density of nucleation on the substrate surface depends on the manner of deposition, being greater for the step-by-step approach i.e. at very low deposition rate.

Raman scattering spectra taken from a series of CdS and a series of CdSe layers having thickness in the ranges 30-200 nm and 40-100 nm, respectively are presented in Fig. 5. In the CdSe series only the '50 nm' sample was step-by-step deposited, the other three were one-step prepared. It is seen that, as expected, the intensity of the 1LO (longitudinal optical) band of CdS layers, with peak at ~300 cm^{-1} [21] and gradually increases with layer thickness. In contrast, the 1LO band of CdSe peaked at ~207 cm^{-1} [22] shows a non-monotonous variation when the layer thickness increases. The most important result is that the band intensity from the '50 nm' layer at its maximum is 5 times greater than in the 100 nm sample. This observation can be attributed to resonant absorption of the 647.1 nm light at least in some crystals of the '50 nm' layer whose optical band gap is equal to the energy of the exciting light i.e. greater than the gap of bulk CdSe. Assuming

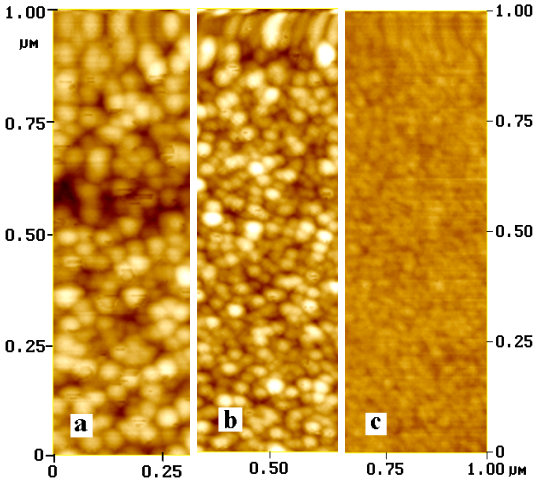

Fig. 4. Two-dimensional AFM images of three CdSe layers having thickness of 50nm prepared using on-step (a - V_d=2.5 nm/s, b - V_d=0.5 nm/s) and s tep-by-step (c-V_d=0.5 nm/s) deposition.

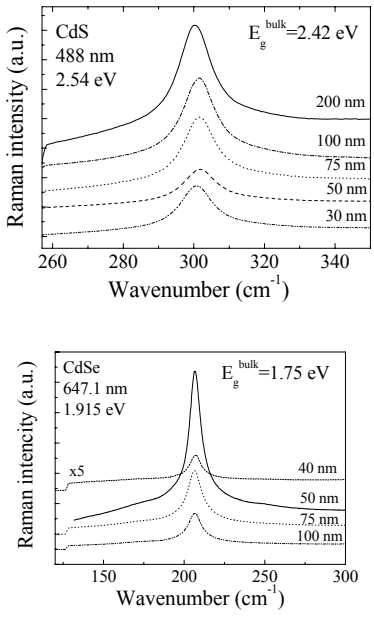

Fig. 5. Raman scattering spectra of a series of CdS and a series of CdSe layers whose thickness is given in the figures. The wavelength and energy of the exciting light as well as the optical band gap of each material at the measurement temperature (295 K) are also indicated in the corresponding figure.

three-dimensional confinement and spherical shape of those grains their diameter should be around 8 nm [23], which is quite possible, keeping in mind the AFM results indicating a size of 10-15 nm. The obtained AFM and Raman scattering results on CdSe layers indicate that the highest gas sensitivity can be expected in the '50 nm' step-by-step films deposited at a rate of 0.5 nm/s since these layers are nanostructured and because of this the number of double Schottky potential barriers at the interface of adjacent grains is highest.

The changes in the photocurrent and dark current registered upon exposure of one-step deposited CdSe films to the same gases used for testing CdS layers are given in Table 2. As anticipated, because of its lowest grain size in this group of samples, the '50 nm' layer deposited at the lower rate of 0.5 nm shows a significant dark current increase upon exposure to all gases tested. However, although the microcrocrystal size ofCdSe layers is much smaller than the size of CdS ones, the photocurrent changes are less. A possible explanation of this result can be connected with the fact that the CdSe layers show a lower photocurrent than the CdS ones. This is probably due to a greater ratio of the fast-to-slow recombination centre density in CdSe, which may reduce the effect of the new gas-related recombination centres. As for the observed greater changes of the dark current in CdS layers than in CdSe ones (compare the second parts of Tables 1 and 2),

Table 2. Changes in the steady state photocurrent and dark current of one-step deposited CdSe thin films upon exposure to different gases. The signs (+) and (-) in front of the numbers indicate photocurrent increase or decrease, respectively.

Deposition rate (nm/s)	Layer thickness (nm)	Photocurrent changes %			
		Ammonia	Water	Ethanol	Acetone
0.5	50	+4	-9	0	0
3	50	-7	-19	-18	-16
0.5	100	-	-12	-13	-
3	100	0	0	-2.5	0
		Dark current changes %			
0.5	50	$+1x10^2$	$+4x10^2$	+90	+90
3	50	0	0	0	0
0.5	100	+22	+10	+5	+11
3	100	0	0	-	-

Table 3. Changes in the steady state photocurrent and dark current of step-by-step CdSe thin films upon exposure to different gases. The signs (+) and (-) in front of the numbers indicate photocurrent increase or decrease, respectively.

Deposition rate (nm/s)	Layer thickness (nm)	Photocurrent changes %				
		Ammonia	Water	Ethanol	Acetone	Iodine
0.5	50	+81	+71	+40	+93	+69
0.5	100	+22	+10	+5.5	+11	
		Dark current changes %				
0.5	50	$+9x10^2$	$+2x10^3$	$+4x10^3$	$+1x10^3$	$+5x10^2$
0.5	100	+32	+30	+25	+21	

it seems that the height of the intergrain barriers in CdS layers is higher and more sensitive to adsorbed gas atoms or molecules. A significant diminution of these barries will result in a greater I_d increase in CdS than that in CdSe.

The changes observed in the photocurrent and dark current upon gas exposure of step-by-step deposited CdSe films are given in Table 3. Considering the photocurrent changes, one can see that in the '50 nm' sample thse changes are greater than in both CdS and one-step CdSe layers. Moreover, the step-by-step CdSe layers show a significant dark current increase upon exposure to all gases tested.This observation can be attributed to the very small grain size (~10-15 nm) determined from the above described AFM (Fig. 4c) and Raman scattering data.

4. Conclusions

Thin films of CdS and CdSe having thickness in the range 30-200 nm and 10-100 nm, respectively, have been prepared by physical vapour deposition. Two deposition approaches have been used: one-step deposition for production of a series of CdS and a series of CdSe layers or step-by-step deposition for production of a series of CdSe layers.

Atomic force microscopy measurements have been performed in order to investigate the effect of the deposition conditions (substrate temperature and deposition rate) on the microcrystal size. They have revealed that in the three groups of samples studied the grain size appreciably decreases with decreasing layer thickness and this effect is strongest in the step-by-step CdSe layers. Moreover, at the same layer thickness, the microcrystal size in CdS layers is greater than in CdSe layers, attributed to the higher deposition temperature (150 ^oC) of CdS layers than that of CdSe (30 ^oC). The strong size decrease in the step-by-step CdSe group is related to the combination of an extremely small average deposition rate and low deposition temperature. Raman scattering measurements carried out at room temperature have shown an expected gradual increase of the scattered

light from CdS layers with increasing layer thickness. However, a non-monotonous change in the CdSe group is seen, in which the intensity is strongest for the '50 nm' 'step-by-step' CdSe layer. This observation is ascribed to a size-induced increase of the optical band gap of a part of the microcrystals in those layers whose size has been estimated to be ~ 8 nm. The Raman data are in good agreement with the nanocrystal size (10-15 nm) determined from the AFM results.

Room temperature investigations have been performed on the effect of exposure to a set of vapours (water, ethanol, ammonia, iodine and acetone in air) on the dc dark and steady state photoconductivity of layers. The CdS layers have shown a strong change of the dark current and reasonable change of the photocurrent of all CdS layers exposed to water vapour. The response to the other vapours is rather weak; it increases with decreasing layer thickness. None of the CdSe layers have shown good sensitivity to all vapours used with the exception of the 50 nm layers as the 'step-by-step' layer shows the highest sensitivity to water vapour, ethanol, ammonia, iodine and acetone vapours. The observed relatively high gas-sensitivity of 'step-by-step' CdSe layers has been related to the greatest integral interface area between nanocrystals in these layers than in thicker and the 'one-step' layers. These preliminary results on the gas sensitivity of 'step-by-step' deposited CdSe layers are a useful basis for the study of gas-sensor applications of CdS and CdSe.

Acknowledgements

This work was supported jointly by NATO through a Collaborative Linkage Grant PST.CLG.980656 and the Bulgarian Ministry of Education and Science under grant F-1306.

References

[1] G. Sberveglieri (ed.), Gas Sensors, Kluwer, Dordrecht Germany (1992).
[2] T. Vossmeyer, H. Tomita, Sony International Patent, EP1039291 (2000).
[3] T. Vossmeyer, US patent **6** (458), 327 (2002).
[4] A. C. R. Pipino, US Patent **6** (515), 749 (2003).
[5] Ch.-Y. Chen, Ch.-T. Cheng, Ch.-W. Lai, P.-W. Wu, K.-Ch. Wu, Pi-Tai Chou, Yi-H. Chou, H.-T. Chiu, Chem. Commun. **2006**, 263 (2006).
[6] Y. Sh. Kim, S. -Ch. Ha, K. Kim, H. Yang, S. -Y Cho, Y. T. Kim, J. T. Park, Ch. H. Lee, J. Ch. J. Paek, K. Lee, Appl. Phys. Lett. **86**, 213105 (2005).
[7] Y. Imb, R. P. Vasquezc, Ch. Leec, N. Myungd, R. Penner, M. Yun, Journal of Physics: Conference Series **38**, 61 (2006).
[8] A. K. Prasad, D. J. Kubinski, P. I. Gouma, Sensors and Actuators B **93**, 25 (2003).
[9] R. Martins, E. Fortunato, P. Nunes, I. Ferreira, A. Marques, M. Bender, N. Katsarakis, V. Cimalla, G. Kiriakidis, J.Appl.Phys. **96**, 1398 (2004).
[10] K. K. Makhija, A. Ray, R. M. Patel, U. B. Trivedi, H. N. Kapse, Bull. Mater. Sci. **28**, 9 (2005).
[11] B. K. Miremadi, K. Colbow, Y. Harima, Rev. Sci. Instrum. **68**, 3898 (1997).
[12] S. A. Filonovich, Y. P. Rakovich, A. G. Rolo, M. V. Artemyev, G. Hungerford, M. I Vasilevskiy, M. J. M. Gomes, J. F. M. Ferreira, J. Optoelectron. Adv. Mater. **2**, 623 (2000).
[13] M. Patel, C.-J. J. Pu, L. R. Sharpe, Langmuir **11**, 2003 (1995).
[14] V. A. Smyntyna, V. Gersutenko, S. Sashulis, G. Mattogno, S. Reghini, Sensors and Actuators B **18-19**, 464 (1994).
[15] R. K. Srivastava, P. Lal, R. Dwivedi, S. K. Srivastatva, Sens. Actuators B **21**, 213 (1994).
[16] B. Timmer, W. Olthuis, A. van den Berg, Sensors and Actuators B **107**, 666 (2005).
[17] D. Nesheva, D. Arsova, Z. Levi, Phil. Mag. B **70**, 205 (1994).
[18] D. Nesheva, Z. Levi, Semicond. Sci. Technol. **12**, 1319 (1997).
[19] D. Nesheva, A. G. Fitzgerald, C. Main, Z. Aneva, S. Reynolds, *to be published*.
[20] K. L. Chopra, Electrical phenomena in thin films, ed. T. D. Shermergor, Mir, Moskva (1972) p. 11.
[21] A. Balandin, K. L. Wang, N. Kouklin, S. Bandyopadhyay, Appl.Phys. Lett. **76**, 137 (2000).
[22] D. Nesheva, C. Raptis, Z. Levi, Phys. Rev. B **58**, 7913 (1998).
[23] V. I. Klimov, in Handbook of Nanostructured Materials and Nanotechnology, ed. H. S. Nalwa, Academic Press, San Diego (2000), vol. **4**, chapter 7.

Corresponding author's e-mail: nesheva@issp.bas.bg